Cortical Surface Complexity in Frontal and Temporal Areas Varies Across Subgroups of Schizophrenia

Igor Nenadic*, Rachel A. Yotter, Heinrich Sauer, and Christian Gaser

Department of Psychiatry and Psychotherapy, Jena University Hospital, Friedrich Schiller University Jena, Jena, Germany

Abstract: Schizophrenia is assumed to be a neurodevelopmental disorder, which might involve disturbed development of the cerebral cortex, especially in frontal and medial temporal areas. Based on a novel spherical harmonics approach to measuring complexity of cortical folding, we applied a measure based on fractal dimension (FD) to investigate the heterogeneity of regional cortical surface abnormalities across subgroups of schizophrenia defined by symptom profiles. A sample of 87 patients with DSM-IV schizophrenia was divided into three subgroups (based on symptom profiles) with predominantly negative ($n = 31$), disorganized ($n = 23$), and paranoid ($n = 33$) symptoms and each compared to 108 matched healthy controls. While global FD measures were reduced in the right hemisphere of the negative and paranoid subgroups, regional analysis revealed marked heterogeneity of regional FD alterations. The negative subgroup showed most prominent reductions in left anterior cingulate, superior frontal, frontopolar, as well as right superior frontal and superior parietal cortices. The disorganized subgroup showed reductions in bilateral ventrolateral/orbitofrontal cortices, and several increases in the left hemisphere, including inferior parietal, middle temporal, and midcingulate areas. The paranoid subgroup showed only few changes, including decreases in the right superior parietal and left fusiform region, and increase in the left posterior cingulate cortex. Our findings suggest regional heterogeneity of cortical folding complexity, which might be related to biological subgroups of schizophrenia with differing degrees of altered cortical developmental pathology. *Hum Brain Mapp 00:000–000, 2013*.

Key words: cerebral cortex; cortical folding; fractal dimension; magnetic resonance imaging; psychosis; psychopathology; schizophrenia

INTRODUCTION

The conceptualization of schizophrenia as a neurodevelopmental disorder has built on several lines of research converging on mechanisms related to (subtle) disturbance of brain development as a major pathogenetic factor [Arnold et al., 2005; Church et al., 2002; Marenco and Weinberger, 2000]. This has included neuropathological studies, which—in the absence of astrogliosis as a hallmark feature of neurodegeneration—have found subtle abnormalities of neuronal migration in medial temporal lobe areas such as the entorhinal cortex [Falkai et al., 2000; Jakob and Beckmann, 1986], as well as the

Contract grant sponsor: BMBF; Contract grant numbers: BMBF 01EV0709 and 01GW0740 (C.G.); Contract grant sponsor: Friedrich Schiller University of Jena; Contract grant number: DRM 21007087 (I.N.)

*Correspondence to: Igor Nenadic, Department of Psychiatry and Psychotherapy, Jena University Hospital, Philosophenweg 3, 07743 Jena, Germany. E-mail: igor.nenadic@uni-jena.de

Received for publication 4 September 2012; Revised 9 January 2013; Accepted 14 February 2013

DOI: 10.1002/hbm.22283

Published online in Wiley Online Library (wileyonlinelibrary.com).

parahippocampal gyrus and prefrontal cortex [Eastwood and Harrison, 2005]. Current evidence points to several mechanisms that may cause subtle impairment in cortical development in schizophrenia, including both genetic and adverse environmental factors [Hyde et al., 2011; Kang et al., 2011; Lodge and Grace, 2011].

Assessment of the folding of the cerebral cortex has therefore become of particular interest to study the sequelae of cortical developmental pathologies. Most structural brain imaging studies on alterations of grey matter in the cortex in schizophrenia have relied on techniques such as regional volumetry or voxel-based morphometry (VBM). While these methods have been used to establish a pattern of structural alterations [Bora et al., 2011], they probably reflect a mixture of effects including genuinely pathogenetic mechanisms, as well as changes occurring during transition to psychosis or later during the disease, related to disease progression, medication, or even short-term clinical changes such as occurrence of a psychotic episode. More recent morphometric studies have relied on the application of cortical surface-based measurements, including those of cortical thickness, cortical folding, and gyrification. The latter is of particular interest, because it is assumed to reflect a marker that is temporally stable over most of the adult human life span and probably reflects changes related to the neurodevelopmental origins of the disorder. Several of the recently published studies on gyrification and cortical complexity, for example, report changes in the prefrontal cortex [Narr et al., 2004; White and Hilgetag, 2011; Yotter et al., 2011]. The overlap of the mentioned neuropathological post mortem and in vivo brain imaging studies, therefore, underline the hypothesis that imaging markers of cortical complexity might provide information related to disturbed brain development and the emergence of cortical folding. Such structural effects on cortical folding might then relate to functional pathologies of connectivity [White and Hilgetag, 2011]. Also, recent findings suggest a genetic impact on (frontal) gyrification in families affected with schizophrenia [Falkai et al., 2007]. However, schizophrenia can manifest at different stages of brain development (late childhood, adolescence, or adulthood), and it also shows considerable heterogeneity of clinical phenotype, disease course, as well as genetic load in different patients. Therefore, subtle pathologies of cortical development might not only affect different brain areas to different extents but also might vary across patient populations. This assumption has also served to explain phenotypic variation across the spectrum of psychosis [Murray et al., 2004; Nenadic et al., 2012a].

In the present study, we test the hypothesis that disturbed cortical complexity varies across subgroups of schizophrenia patients, reflecting differential involvement of early developmental impacts. We applied a novel and recently validated method assessing cortical surface complexity based on a spherical harmonics approach [Yotter et al., 2011] to study fractal dimensional (FD) measures in subgroups of a large schizophrenia sample. The rationale was to identify cortical areas where this surface measure (a putative marker of early neurodevelopmental alterations) might converge across all groups, and where it might show variability depending on the subgroup. For delineation of subgroups, we used an approach based on psychopathology, which had been applied in two recent large VBM studies investigating variability of brain structural changes across subgroups of the disease [Koutsouleris et al., 2008; Nenadic et al., 2010].

METHODS

Subjects and Subgroup Formation

We included a total of 87 patients with DSM-IV schizophrenia (48 males and 39 females; mean age 35.5 years, SD 10.96) and 108 healthy controls (68 males and 40 females; mean age 32.16 years, SD 9.99). All subjects had given written informed consent to a study protocol approved by the ethics committee of the University of Jena Medical School. The present sample is a subsample of a previous morphometric study, initially including 99 patients and 113 healthy controls, for which we have previously published VBM analyses, and where clinical details have been reported in more detail [Nenadic et al., 2010, 2012b]. In addition to meeting DSM-IV criteria for schizophrenia, patients also met DSM-IIIR criteria for chronic disease, i.e., disease duration of more than 2 years. None of the participants had any neurological or major medical condition, including traumatic brain injury, which might affect morphometric measures, and all subjects were right handed [Oldfield, 1971]. All patients were on stable antipsychotic medication and had stable clinical symptoms.

Subgroups were formed using a factor analysis approach with Promax rotation considering the commonly proposed three-factor solution [see also (Nenadic et al., 2010]). This three-factor solution has been described in a number of clinical studies, and can be replicated even in old-age samples, supporting its validity across the life span [Sauer et al., 1999]. All patients were assessed for clinical symptoms using the SANS and SAPS rating scales. For subsequent factor analysis, we made use of the full sample of 99 patients, including all single items of the SANS and SAPS scales, which led (after exclusion of a few patients, based on MR image quality as given in detail below) to subgroups of 31, 23, and 33 patients, respectively, for the negative, disorganized, and paranoid subgroups (S1, S2, S3). Demographics of the three subgroups are shown in Table I. The three subgroups did not differ from the healthy control sample with respect to age (overall ANOVA across the four groups; $F = 0.19$; $P = 0.981$; comparison of each subgroup vs. healthy controls using t-tests: S1 vs. HC: $P > 0.135$; S2 vs. HC: $P > 0.208$; S3 vs. HC: $P > 0.126$); also, there was no difference between the distribution of gender comparing each of the subgroups with the healthy controls (overall χ^2 test: χ^2 2.19, df = 1, $P > 0.53$; χ^2 tests of comparisons between each subgroup and controls: S1 vs. HC: χ^2 1.56, df = 1, $P > 0.21$; S2 vs.

TABLE I. Demographic data of the three schizophrenia subgroups and healthy controls

	Negative subgroup (S1)	Disorganized subgroup (S2)	Paranoid subgroup (S3)	Healthy controls (C)
N	31	23	33	108
Females/males	16/15	9/14	14/19	40/68
Mean age (SD)	35.54 (11.17)	35.39 (11.13)	35.54 (11.18)	32.16 (9.99)
Age range	18.45–54.54	19.80–59.16	19.22–64.96	20.0–59.44
SAPS mean total score (SD)	11.5 (11.7)	24.3 (14.0)	22.6 (18.9)	N/A
SANS mean total score (SD)	44.6 (14.1)	35.7 (16.5)	27.8 (17.8)	N/A

HC: χ^2 0, df = 1, $P = 1$; S3 vs. HC: χ^2 0.12, df = 1, $P > 0.72$).

Image Acquisition Protocol and Cortical Surface Extraction

High-resolution T_1-weighted anatomical magnetic resonance images (MRI) were acquired on a 1.5-T Phillips Gyroscan ASCII system covering the entire brain [256 sagittal slices, 1 × 1 × 1 mm voxels; TR 13 ms, TE 5 ms, a 25°, field of view (FOV) 256 mm]. Head movement was restricted using foam pads. Images were both visually inspected for artifacts and then using an automated quality check implemented in the VBM8 package (http://dbm.neuro.uni-jena.de/vbm8). While all of the initially scanned 99 patients and 113 healthy controls passed this quality control, we excluded 12 patients and 5 healthy controls based on poor quality of cortical surface reconstruction (as rated with an internal scoring system).

Cortical surfaces were extracted using mostly automated procedures from the FreeSurfer v.4.5 software suite (http://surfer.nmr.mgh.harvard.edu). Briefly, images were intensity normalized, skull-stripped, aligned for head position along the commissural axis, and finally labeled for cortical and subcortical structures [Dale et al., 1999; Fischl et al., 1999a,b]. To segment the images, they were first rigid-body registered to a probabilistic brain atlas, then morphed nonlinearly to the atlas. Each voxel was then assigned to one specific tissue glass (gray matter, white matter, CSF, or background) depending on its location, the intensity, and local spatial configuration [Fischl and Dale, 2000].

To obtain a surface mesh, the white matter tissue segmentation map was processed using the marching cubes algorithm, then corrected to repair any topological defects. By outwardly deforming the white matter surface, the pial surface was also generated [Dale et al., 1999; Fischl and Dale, 2000]. As a final step, the pial and white matter surfaces were averaged together, vertex by vertex, to construct a central surface. The central surface meshes were then used as the input for complexity analysis.

Derivation of Cortical Complexity Maps

Cortical complexity was calculated using a recently published and validated method to quantify local FD using spherical harmonic reconstructions [Yotter et al., 2011]. Compared to standard FD derivations, which is generally a regression of log(area) versus log(dimension) over a certain range of scales, the spherical harmonic approach regresses log(area) versus the maximum l value (or degree) of the reconstruction. Using this approach, complexity may be calculated at different scales: global, regional, and local. The global complexity is a single value for the entire hemisphere; regional or local values are a set of values for regions of interest or vertices, respectively. This method overcomes limitations of previous applications of FD measures applied across an entire hemisphere only [Ha et al., 2005].

For each hemisphere, we extracted the spherical harmonic coefficients of the central surface up to a maximum l value of 1024. The spherically remapped points were transformed into harmonic space using a modification of the fast Fourier transform [Kostelec et al., 2000], and 10 reconstructions were derived using maximum l values between 11 and 29. FD is calculated by finding the slope of the linear portion of the log-log plot of area versus maximum l value.

TABLE II. Comparison of mean fractal dimension (FD) values across the left and right hemisphere (*P* values of *t*-test comparison vs. respective hemisphere values in healthy controls given in right column)

Groups	Hemisphere	Global FD ± SEM	*P* (*t*-test comparing group vs. C)
Healthy controls (C)	Left	2.5820 ± 0.0002	
	Right	2.5871 ± 0.0003	
Negative schizophrenia subgroup (S1)	Left	2.5769 ± 0.0007	0.3160
	Right	2.5647 ± 0.0008	**0.00016**[a]
Disorganized schizophrenia subgroup (S2)	Left	2.5891 ± 0.0010	0.2213
	Right	2.5822 ± 0.0012	0.4616
Paranoid schizophrenia subgroup (S3)	Left	2.5738 ± 0.0010	0.1377
	Right	2.5741 ± 0.0009	**0.0277**[a]

[a] $P < 0.05$.

TABLE III. Region-of-interest (ROI)-based analysis of cortical complexity (fractal dimensions, FD) in healthy controls (C) and subgroups of schizophrenia (S1: negative group; S2: disorganized group; S3: paranoid group)

	Left hemisphere ROI				Right hemisphere ROI			
	C	S1	S2	S3	C	S1	S2	S3
Bankssts	2.815	**2.728**[b]	2.796	2.816	2.880	**2.822**[b]	2.872	2.853
Caudal ant. cingulate	2.295	**2.165**[c]	2.302	2.281	2.063	**2.019**[b]	2.059	2.051
Caudal middle frontal	2.734	2.750	2.758	2.696	2.676	2.647	2.687	2.656
Corpus callosum	2.176	**2.145**[b]	2.168	2.178	2.548	2.515	2.528	**2.497**[b]
Cuneus	2.651	**2.713**[a]	**2.734**[a]	2.659	2.721	2.754	2.746	2.760
Entorhinal	2.903	2.977	2.909	2.878	2.339	2.352	2.350	2.342
Fusiform	2.530	2.557	2.487	**2.481**[b]	2.473	2.459	2.473	2.467
Inferior parietal	2.692	2.719	**2.733**[a]	2.668	2.645	**2.596**[b]	2.672	2.624
Inferior temporal	2.469	2.471	2.487	2.447	2.527	2.503	2.519	2.540
Isthmus cingulate	2.185	**2.227**[a]	**2.224**[a]	2.215	2.749	2.703	2.750	2.780
Lateral occipital	2.505	2.505	2.528	2.496	2.480	2.482	2.503	2.469
Lateral orbitofrontal	2.267	2.284	**2.298**[a]	2.274	2.356	2.344	2.362	2.351
Lingual	2.600	2.577	2.583	2.588	2.684	2.659	**2.630**[b]	2.647
Medial orbitofrontal	2.421	2.454	2.426	2.457	2.398	2.390	2.395	2.393
Middle temporal	2.678	2.688	**2.732**[a]	2.654	2.880	2.867	**2.922**[a]	2.887
Parahippocampal	2.908	2.943	2.917	2.883	2.535	2.500	2.513	2.496
Paracentral	2.478	2.491	**2.516**[a]	2.502	2.902	2.922	2.906	2.878
Pars opercularis	2.761	2.757	2.747	2.742	2.185	2.184	2.207	2.201
Pars orbitalis	2.965	**2.895**[b]	3.006	2.987	2.290	2.300	**2.246**[b]	2.295
Pars triangularis	2.777	2.741	2.749	2.747	2.539	2.550	2.515	2.548
Pericalcarine	2.580	**2.515**[b]	2.561	2.581	2.857	**2.796**[b]	2.897	2.851
Postcentral	2.771	2.758	2.766	2.740	2.498	2.513	2.521	2.500
Posterior cingulate	2.436	**2.482**[a]	2.476	**2.489**[a]	2.468	2.477	**2.426**[b]	2.458
Precentral	2.730	**2.678**[c]	2.727	2.727	2.584	**2.563**[b]	2.571	2.572
Precuneus	2.564	**2.522**[b]	2.558	2.561	2.714	2.683	2.685	2.695
Rostral ant. cingulate	2.113	2.078	2.122	2.100	2.312	2.320	2.328	2.301
Rostral middle frontal	2.585	2.611	2.589	2.582	2.585	2.562	2.594	2.581
Superior frontal	2.381	**2.345**[c]	2.373	2.373	2.753	**2.724**[b]	2.763	2.750
Superior parietal	2.667	2.643	2.684	2.649	2.733	**2.647**[c]	2.712	**2.657**[c]
Superior temporal	2.787	2.770	2.775	2.765	2.448	2.431	2.440	2.445
Supramarginal	2.626	2.633	2.628	2.608	2.444	2.435	2.431	2.450
Frontal pole	2.795	**2.724**[b]	2.763	2.768	3.181	3.247	3.258	3.163
Temporal pole	2.811	2.855	2.844	2.777	2.550	**2.618**[a]	2.570	2.546
Transverse temporal	2.642	**2.887**[a]	**2.733**[a]	2.706	1.958	1.978	1.963	1.966

[a]Significant reduction ($P < 0.05$, uncorrected).
[b]Significant increase ($P < 0.05$, uncorrected).
[c]Significant reduction ($P < 0.05$, FDR correction).

Calculation of the global complexity value was obtained directly from the total surface area of the reconstructions. Locally, complexity values for each polygon were estimated by regressing the log–log plot of normalized area of the polygon versus the maximum l value, and pointwise complexity values were the average of complexity values for all neighboring polygons.

For intersubject comparisons, local complexity maps were re-parameterized into a common coordinate system. This was accomplished using the registered spherical mapping for each subject (*xh.sphere.reg*), then re-parameterizing the local complexity values using the *fsaverage* spherical mesh included in FreeSurfer. These values were then smoothed using a 30-mm Gaussian heat kernel [Chung et al., 2005]. Regional values were obtained by averaging the complexity values associated with a particular region of interest.

Statistical Analysis

Our main analysis was carried out on two levels: global and regional (i.e., across atlas-defined ROIs). Hence, we first considered a *t*-test for global left and right hemisphere FD values, respectively. Then, we tested regional differences for each of the atlas-defined ROIs using a general linear model; based on our anatomical hypotheses derived from our previous finding of FD in schizophrenia [Yotter et al., 2011] as well as related findings on cortical surface parameters, which indicate disease-related alterations in prefrontal

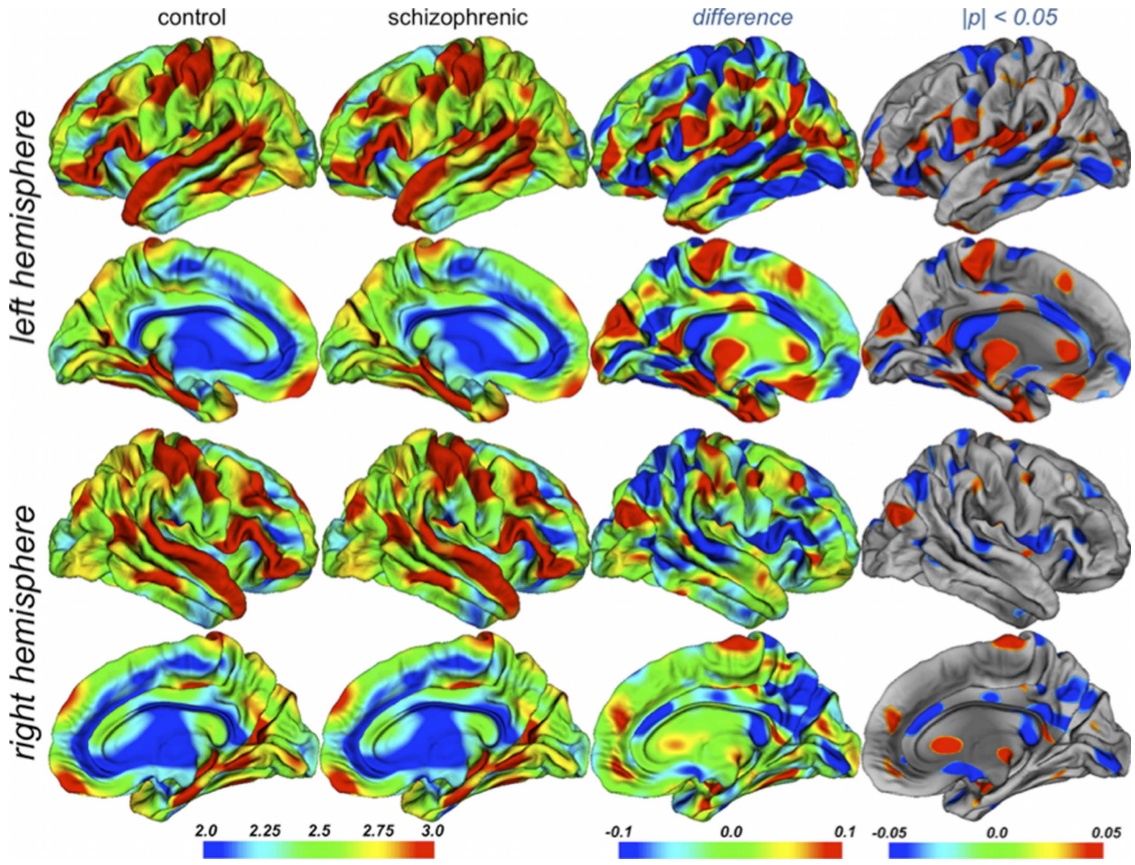

Figure 1.

Comparison of local cortical complexity (fractal dimensions, FD) between healthy controls and schizophrenia subgroup 1 (predominantly negative symptoms) with projections of vertexwise values of (columns from left to right): (**a**) the healthy control group, (**b**) subgroup 1, (**c**) the mean difference between the two groups, and (**d**) the statistical significance maps (blue indicating significantly lower, red indicating significantly higher FD values). [Color figure can be viewed in the online issue, which is available at wileyonlinelibrary.com.]

and temporal regions, we defined a threshold of $P = 0.05$. In addition to these analyses based on a priori anatomical hypotheses, we performed an additional confirmatory analysis to indicate which of the ROIs would survive correction for multiple comparisons using the false discovery rate (FDR) method [Benjamini and Hochberg, 1995].

Finally, we carried out a third set of analyses, which was an exploratory analysis of FD values in subgroups at the vertex level, i.e., comparing FD values in each of the vertices across each hemisphere for each subgroup against healthy controls. For this exploratory analysis, a threshold of $P < 0.05$ was applied. This analysis was intended to complement the above in that it shows changes with greater resolution; however, this analysis is only complementary as it highly increases the number of multiple comparisons made, hence rendering it likely to be underpowered for corrected statistical thresholds—especially given that our subgroup approach divided the patient cohort in smaller groups.

RESULTS

For the analysis of global hemispherical FD, we found a significant difference in the right hemisphere between both the negative and paranoid subgroups compared to healthy controls, but not for the disorganized subgroup or for the left hemisphere in any of the three subgroups. Mean global FD values are given in Table II.

For the analysis of regional FD, we found several changes, both increases and decreases of FD in frontal and (lateral) temporal, but also parietal areas. All findings are shown in Table III. Of particular interest were reductions of FD in the negative subgroup in the left anterior cingulate, superior frontal, frontopolar, as well as right superior frontal and superior parietal cortical ROIs. Within the disorganized subgroup reductions included bilateral ventrolateral/orbitofrontal cortices, and several increases in the left hemisphere, including inferior parietal, middle temporal, and midcingulate areas. While these analyses were

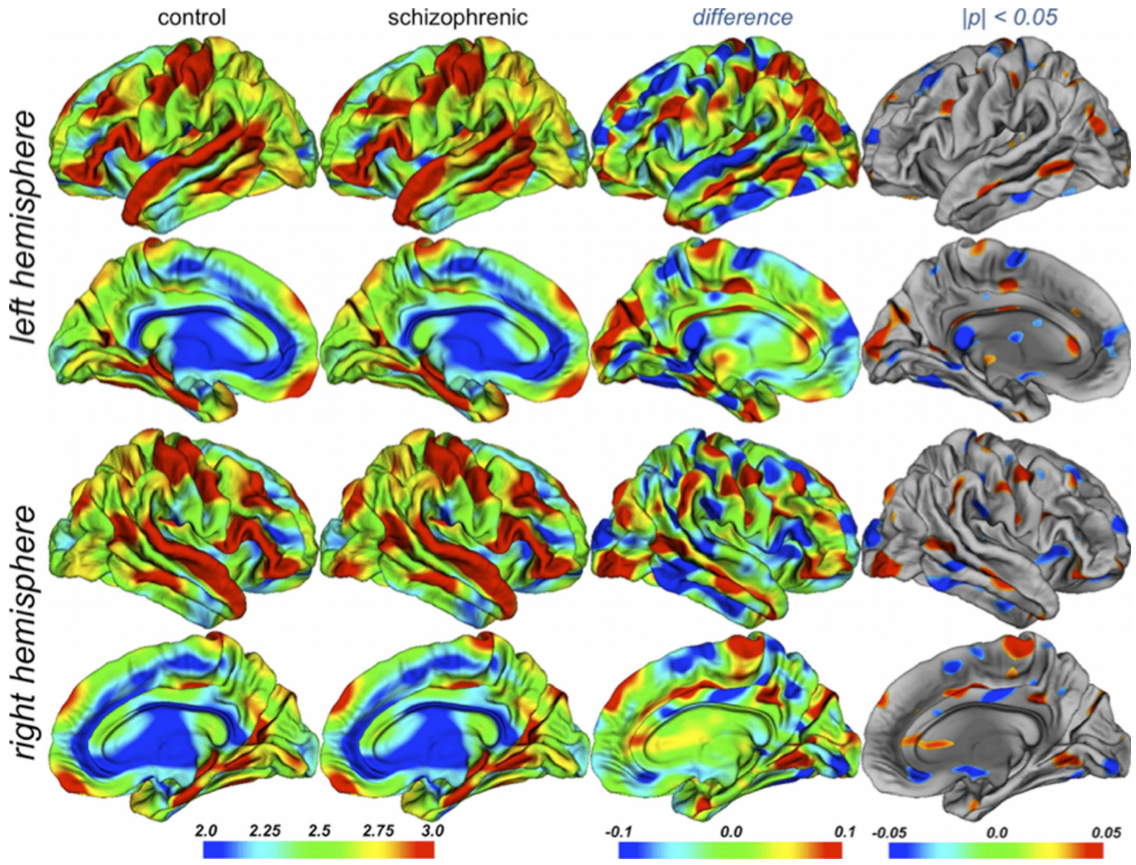

Figure 2.

Comparison of local cortical complexity (fractal dimensions, FD) between healthy controls and schizophrenia subgroup 2 (predominantly disorganized symptoms) with projections of vertex-wise values of (columns from left to right): (**a**) the healthy control group, (**b**) subgroup 2, (**c**) the mean difference between the two groups, and (**d**) the statistical significance maps (blue indicating significantly lower, red indicating significantly higher FD values). [Color figure can be viewed in the online issue, which is available at wileyonlinelibrary.com.]

carried out with a priori anatomical hypotheses, our additional analysis applying FDR correction for multiple comparison showed that some of the findings did actually survive this correction, in particular for the left caudal anterior cingulate, left precentral and left superior frontal ROIS in the negative subgroup, as well as the right superior parietal ROIs in the paranoid and disorganized subgroups (see Table III: green markings).

Finally, by means of an explorative analysis, we provide local FD comparison maps across the cortex (all at a threshold of $P < 0.05$) comparing each of the subgroups with the healthy control sample, i.e., versus the negative subgroup (Fig. 1), disorganized subgroup (Fig. 2), and paranoid subgroup (Fig. 3).

DISCUSSION

In this study, we aimed to test the hypothesis whether a novel FD measure would show convergence on one or few areas across three subgroups of schizophrenia patients, delineated on the basis of cross-sectional psychopathology. Our method allowed us to assess both the global (i.e., hemisphere) as well as regional levels of this new measure of cortical surface complexity. We have demonstrated changes of FD in prefrontal, lateral temporal, anterior and midcingulate, as well as superior parietal areas, which show marked heterogeneity across subgroups. Even though we identified several areas where two of the three subgroups showed changes in the same direction (sometimes with a trend in the third, e.g., the left transverse temporal and right superior parietal regions), there was no ROI where all subgroups showed clear significant convergence.

Our findings suggest that heterogeneity of clinical phenotypes is concomitant with heterogeneity of FD as a cortical surface measure, which is implied to reflect a state-independent marker. We found no strong evidence for one single area affected in all subgroups, which might represent a "core deficit" common to all or most schizophrenia patients. Similar to measures like the gyrification index,

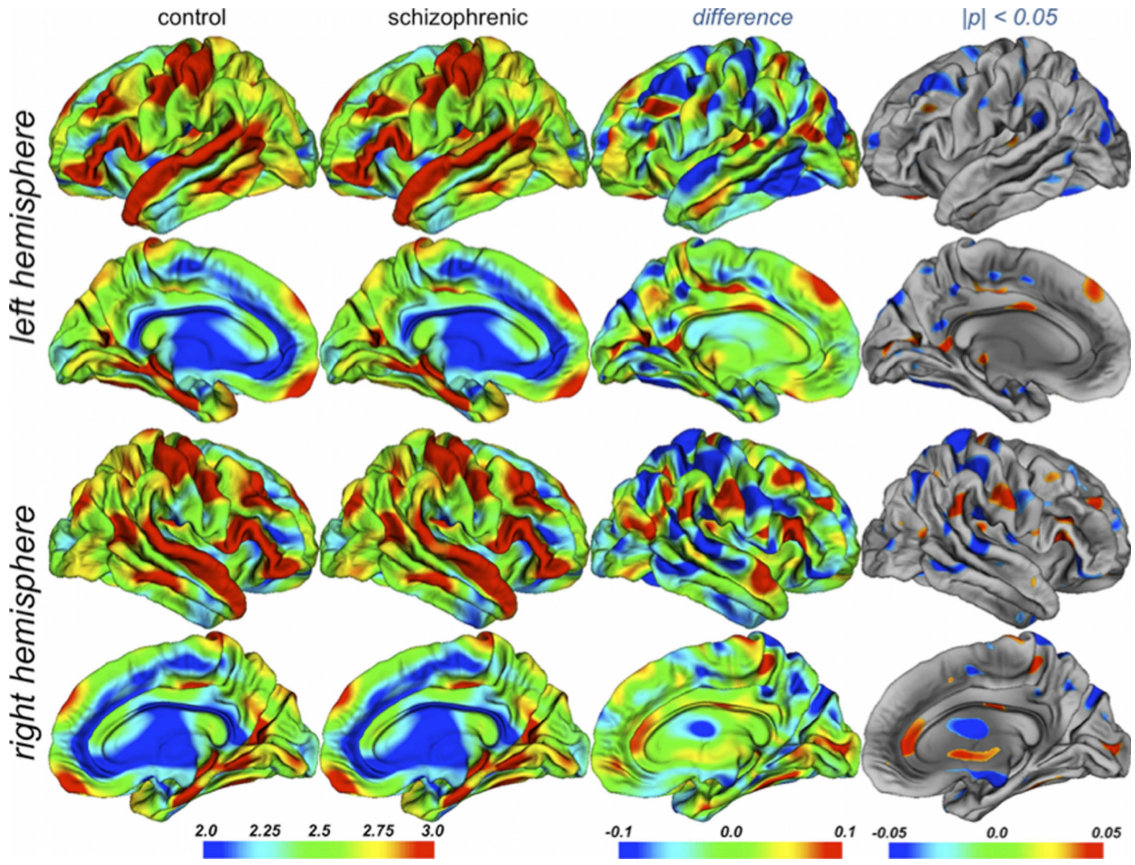

Figure 3.

Comparison of local cortical complexity (fractal dimensions, FD) between healthy controls and schizophrenia subgroup 3 (predominantly paranoid symptoms) with projections of vertexwise values of (columns from left to right): (**a**) the healthy control group, (**b**) subgroup 3, (**c**) the mean difference between the two groups, and (**d**) the statistical significance maps (blue indicating significantly lower, red indicating significantly higher FD values). [Color figure can be viewed in the online issue, which is available at wileyonlinelibrary.com.]

which show changes during intrauterine brain development and in the first years of life, followed by a stable course during most of the life span, our FD measure is based on the complexity of the cortical surface. Changes in this measure would therefore most likely point to early developmental effects that impair brain development and formation of the cerebral cortex. In fact, more recent studies in neonates at the risk of schizophrenia support alterations in both gray and white matter structural parameters [Shi et al., 2012]. Hence, factors most likely influencing these brain structural phenotypes (in contrast to those derived from volumetry or VBM) are genes and early developmental events influencing neuronal migration, establishment of thalamocortical loops, and development of gyri and sulci.

With respect to the regional pattern of changes, three aspects of our study merit particular attention. First, of all the subgroups, the negative group showed the most widespread changes of FD, in particular reductions in the left superior frontal, left anterior cingulate, right superior parietal, and also left precentral ROIs. This is consistent with previous subgroup studies using VBM demonstrating most extensive changes (mostly in the prefrontal cortex) in this group of patients [Koutsouleris et al., 2008; Nenadic et al., 2010]. It therefore appears that the load of neurodevelopmental antecedents of the disorder is largest in these patients, who display few positive psychotic symptoms. Interestingly, the paranoid subgroup, which in previous VBM studies has shown extensive deficits in superior temporal cortices, showed the fewest changes in FD, the only prominent change being a reduction in the right superior parietal region, and less pronounced reduction in the left fusiform, and increase in the left posterior cingulate region.

Second, none of the subgroups of patients showed significant changes in the entorhinal or parahippocampal cortices. This is noteworthy, as most of the neuropathological abnormalities reflecting pathological neuronal migration have been reported in these areas [Eastwood and

Harrison, 2005; Falkai et al., 2000], and there is some corresponding imaging evidence [Qiu et al., 2010]. Hence, even though FD changes might reflect early developmental pathology, they might not necessarily be closely correlated with the above cellular-level changes. A direct comparison of MR-derived cortical surface measures and post mortem neuropathological changes would therefore be necessary to further study this aspect; such data (especially in schizophrenia samples) are not available to our best knowledge. It should be pointed out, however, that this does not contradict a relation of certain neuropathological abnormalities (e.g., interstitial white matter neurons) to cortical surface measures. The development of the gyri in humans is incompletely understood [Toga et al., 2006]. The neuropathological alterations mentioned above might thus be only one of several factors affecting the emergence of a gyral folding pattern, and thus only partially contribute to a cortical surface abnormality detectable with our FD (or related) approaches.

Third, we find evidence for superior parietal cortical pathology in both negative and paranoid subgroups. While one postmortem study has indeed demonstrated evidence for parietal pathology of neuronal development [Kirkpatrick et al., 1999], the anatomical region was slightly more inferior, and we therefore cannot conclude with certainty that this superior parietal pathology might be related to such neuronal pathologies. The parietal cortex, although less frequently implicated in schizophrenia, has been shown to be linked to genetic liability for schizophrenia in twin studies [Hulshoff Pol et al., 2012].

Finally, we need to consider limiting aspects in our study. Our factor analysis approach, although supported by a considerable literature, is inherently limited as it uses clinical data (rather than biological markers) for definition of subgroups. Our study therefore provides a strong indication of biologically distinct subgroups, but further replication and extension would be needed dividing the subgroups on the basis of regional FD values. Also, in the absence of a quantifiable measure of genetic susceptibility on the individual level, we cannot exclude that our subgroups themselves might be heterogeneous regarding the level of genetic impact of disease expression. Our findings rest on the assumption that medication, disease progression, or age-related changes do not significantly influence cortical surface-based measures like FD or gyrification.

In conclusion, our findings provide further evidence for the biological heterogeneity of schizophrenia by showing that a novel marker of cortical complexity, which is possibly related to abnormal cortical development, is not only altered across different cortical areas, but also across three phenotypically delineated subgroups of schizophrenia patients.

REFERENCES

Arnold SE, Talbot K, Hahn CG (2005): Neurodevelopment, neuroplasticity, and new genes for schizophrenia. Prog Brain Res 147:319–345.

Benjamini Y, Hochberg Y (1995): Controlling the false discovery rate: a practical and powerful approach to multiple testing. J R Stat Soc Ser B (Methodol) 57:289–300.

Bora E, Fornito A, Radua J, Walterfang M, Seal M, Wood SJ, Yucel M, Velakoulis D, Pantelis C (2011): Neuroanatomical abnormalities in schizophrenia: A multimodal voxelwise meta-analysis and meta-regression analysis. Schizophr Res 127:46–57.

Chung MK, Robbins SM, Dalton KM, Davidson RJ, Alexander AL, Evans AC (2005): Cortical thickness analysis in autism with heat kernel smoothing. NeuroImage 25:1256–1265.

Church SM, Cotter D, Bramon E, Murray RM (2002): Does schizophrenia result from developmental or degenerative processes? J Neural Transm Suppl 63:129–147.

Dale AM, Fischl B, Sereno MI (1999): Cortical surface-based analysis: I. Segmentation and surface reconstruction. NeuroImage 9:179–194.

Eastwood SL, Harrison PJ (2005): Interstitial white matter neuron density in the dorsolateral prefrontal cortex and parahippocampal gyrus in schizophrenia. Schizophr Res 79:181–188.

Falkai P, Honer WG, Kamer T, Dustert S, Vogeley K, Schneider-Axmann T, Dani I, Wagner M, Rietschel M, Muller DJ, Schulze TG, Gaebel W, Cordes J, Schonell H, Schild HH, Block W, Traber F, Steinmetz H, Maier W, Tepest R (2007): Disturbed frontal gyrification within families affected with schizophrenia. J Psychiatr Res 41:805–813.

Falkai P, Schneider-Axmann T, Honer WG (2000): Entorhinal cortex pre-alpha cell clusters in schizophrenia: Quantitative evidence of a developmental abnormality. Biol Psychiatry 47:937–943.

Fischl B, Dale AM (2000): Measuring the thickness of the human cerebral cortex from magnetic resonance images. Proc Natl Acad Sci USA 97:11050–11055.

Fischl B, Sereno MI, Dale AM. (1999a): Cortical surface-based analysis: II: Inflation, flattening, and a surface-based coordinate system. NeuroImage 9:195–207.

Fischl B, Sereno MI, Tootell RBH, Dale AM. (1999b): High-resolution intersubject averaging and a coordinate system for the cortical surface. Hum Brain Mapp 8:272–284.

Ha TH, Yoon U, Lee KJ, Shin YW, Lee JM, Kim IY, Ha KS, Kim SI, Kwon JS (2005): Fractal dimension of cerebral cortical surface in schizophrenia and obsessive-compulsive disorder. Neurosci Lett 384:172–176.

Hulshoff Pol HE, van Baal GC, Schnack HG, Brans RG, van der Schot AC, Brouwer RM, van Haren NE, Lepage C, Collins DL, Evans AC, Boomsma DI, Nolen W, Kahn RS (2012): Overlapping and segregating structural brain abnormalities in twins with schizophrenia or bipolar disorder. Arch Gen Psychiatry 69:349–359.

Hyde TM, Lipska BK, Ali T, Mathew SV, Law AJ, Metitiri OE, Straub RE, Ye T, Colantuoni C, Herman MM, Bigelow LB, Weinberger DR, Kleinman JE (2011): Expression of GABA signaling molecules KCC2, NKCC1, and GAD1 in cortical development and schizophrenia. J Neurosci 31:11088–11095.

Jakob H, Beckmann H (1986): Prenatal developmental disturbances in the limbic allocortex in schizophrenics. J Neural Transm 65:303–26.

Kang E, Burdick KE, Kim JY, Duan X, Guo JU, Sailor KA, Jung DE, Ganesan S, Choi S, Pradhan D, Lu B, Avramopoulos D, Christian K, Malhotra AK, Song H, Ming GL (2011): Interaction between FEZ1 and DISC1 in regulation of neuronal development and risk for schizophrenia. Neuron 72:559–571.

Kirkpatrick B, Conley RC, Kakoyannis A, Reep RL, Roberts RC (1999): Interstitial cells of the white matter in the inferior parietal cortex in schizophrenia: An unbiased cell-counting study. Synapse 34:95–102.

Kostelec PJ, Maslen DK, Dennis M, Healy J, Rockmore DN (2000): Computational harmonic analysis for tensor fields on the two-sphere. J Comput Phys 162:514–535.

Koutsouleris N, Gaser C, Jager M, Bottlender R, Frodl T, Holzinger S, Schmitt GJ, Zetzsche T, Burgermeister B, Scheuerecker J, Born C, Reiser M, Moller HJ, Meisenzahl EM (2008): Structural correlates of psychopathological symptom dimensions in schizophrenia: A voxel-based morphometric study. Neuroimage 39:1600–1612.

Lodge DJ, Grace AA (2011): Developmental pathology, dopamine, stress and schizophrenia. Int J Dev Neurosci 29:207–213.

Marenco S, Weinberger DR (2000): The neurodevelopmental hypothesis of schizophrenia: Following a trail of evidence from cradle to grave. Dev Psychopathol 12:501–527.

Murray RM, Sham P, Van Os J, Zanelli J, Cannon M, McDonald C (2004): A developmental model for similarities and dissimilarities between schizophrenia and bipolar disorder. Schizophr Res 71:405–416.

Narr KL, Bilder RM, Kim S, Thompson PM, Szeszko P, Robinson D, Luders E, Toga AW (2004): Abnormal gyral complexity in first-episode schizophrenia. Biol Psychiatry 55:859–867.

Nenadic I, Gaser C, Sauer H (2012a): Heterogeneity of brain structural variation and the structural imaging endophenotypes in schizophrenia. Neuropsychobiology 66:44–49.

Nenadic I, Sauer H, Gaser C (2010): Distinct pattern of brain structural deficits in subsyndromes of schizophrenia delineated by psychopathology. Neuroimage 49:1153–1160.

Nenadic I, Sauer H, Smesny S, Gaser C (2012b): Aging effects on regional brain structural changes in schizophrenia. Schizophr Bull 38:838–844.

Oldfield RC (1971): The assessment and analysis of handedness: The Edinburgh inventory. Neuropsychologia 9:97–113.

Qiu A, Tuan TA, Woon PS, Abdul-Rahman MF, Graham S, Sim K (2010): Hippocampal-cortical structural connectivity disruptions in schizophrenia: An integrated perspective from hippocampal shape, cortical thickness, and integrity of white matter bundles. Neuroimage 52:1181–1189.

Sauer H, Hornstein C, Richter P, Mortimer A, Hirsch SR (1999): Symptom dimensions in old-age schizophrenics. Relationship to neuropsychological and motor abnormalities. Schizophr Res 39:31–38.

Shi F, Yap PT, Gao W, Lin W, Gilmore JH, Shen D (2012): Altered structural connectivity in neonates at genetic risk for schizophrenia: A combined study using morphological and white matter networks. Neuroimage 62:1622–1633.

Toga AW, Thompson PM, Sowell ER (2006): Mapping brain maturation. Trends Neurosci 29:148–159.

White T, Hilgetag CC (2011): Gyrification and neural connectivity in schizophrenia. Dev Psychopathol 23:339–352.

Yotter RA, Nenadic I, Ziegler G, Thompson PM, Gaser C (2011): Local cortical surface complexity maps from spherical harmonic reconstructions. NeuroImage 56:961–973.